Batteries & Supercaps

Research Article
doi.org/10.1002/batt.202500092

Chemistry Europe
European Chemical Societies Publishing

www.batteries-supercaps.org

Measuring Method of Electrochemically Active Surface Area in All-Solid-State Lithium-Ion Batteries

Toshiyuki Ohashi* and Hironori Kobayashi

A simple electrolyte/electrode interface using a thin film of active material in cathode is constructed to enable measurement of electrochemically active surface area (ECSA) in all-solid-state batteries. The correlation between specific capacitance and specific surface area at the interface is investigated. The correlation has a linear relationship and give a calibration curve. Using the calibration curve as a clue, ECSA of a composite electrode is quantitatively determined from the specific capacitance of the composite cell obtained using electrochemical impedance spectroscopy.

1. Introduction

The development of automotive batteries as an alternative energy source to conventional fossil fuels is more prosperous in recent years. On the development of automotive batteries, prediction of battery performance is important.[1] If the performance of large automotive batteries to that of small lab-scale batteries is predicted using a computational simulation, development costs and period of trial manufacture can be reduced. Some input parameters for the computational simulation are obtained from physical properties of materials, thermodynamic, and electrochemical theories. Other parameters are provided by individual analyzes using a commercial instrument. However, some important parameters for which measurement techniques are not established remain though it is related to battery performance directly. One such important parameter is electrochemically active surface area (ECSA) in electrodes.

As a method for measuring ECSA, the carbon monoxide gas adsorption is known.[2,3] Analytical instruments are commercially available. This method is usually adapted for metal catalysts dispersed on catalyst supports (e.g., carbon materials) used in fuel cells. It utilizes the nature of selective chemisorption on the metal catalyst in contrast to surface area measurement of physical gas adsorption with nitrogen gas (so-called brunauer emmett teller (BET) adsorption method), which is generally performed at low temperatures, and ECSA of the metal catalyst is estimated. However, due to its characteristics, this method is limited to metal catalysts for fuel cells and cannot measure ECSA of battery electrodes such as lithium-ion batteries (LIB).

T. Ohashi
Innovative Research Excellence
Honda R&D Co., Ltd.
1-4-1 Chuo, Wako 351-0193 Saitama, Japan
E-mail: toshiyuki_ohashi@jp.honda

H. Kobayashi
Research Institute of Electrochemical Energy
National Institute of Advanced Industrial Science and Technology (AIST)
1-8-31 Midorigaoka, Ikeda 563-8577 Osaka, Japan

Supporting information for this article is available on the WWW under https://doi.org/10.1002/batt.202500092

Recently, it has been reported that capacitance at the cathode-electrolyte interface of LIB correlates with ECSA, which was applied to a composite electrode containing lithium nickel-manganese-cobalt oxide active materials (NMC) of LIB.[4] They report that the relationship between the mechanical pressure loaded on NMC (particles of NMC are fractured by the pressure) and the capacitance follows the same trend as the relationship between the mechanical pressure on NMC and surface area obtained by krypton gas adsorption (BET adsorption method). In addition, there is a report on the measurement of ECSA focusing on the carbon as conductive agents in sulfur composite electrodes of lithium-sulfur batteries (LIS).[5] In order to estimate the surface area of the carbon conductive agent, the capacitance of interface between the electrolyte and electrode was measured using electrochemical impedance spectroscopy (EIS). Using a typical value of area-normalized capacitance of the carbon material (10 $\mu F\ cm^{-2}$), ECSA of carbon agents was estimated. As described above, there have been a few reports on estimating ECSA of battery electrodes based on the capacitance at the electrolyte-electrode interface in liquid LIB or LIS systems. These two studies[4,5] suggest that the key point is to link the contact area at the electrolyte-active material interface with the capacitance. As shown in **Figure 1**, composite electrodes used in LIB are usually composed of an active electrode material, a binder, and a conducting agent. Furthermore, in case of an all-solid-state battery (ASSB), the composite electrode is formed by premixing the solid electrolyte. If the electrolyte is liquid, measurement by gas adsorption may be effective to a certain degree in estimating the contact area since the liquid is expected to flow into fine spaces (i.e., the voids between particles). However, in case of a solid electrolyte, the interface between the active material and the electrolyte is a solid–solid contact, and it is difficult to estimate the contact area by using gas adsorption measurement. Furthermore, ECSA of these composite electrodes whether electrolyte is liquid or solid are complex and spatially extended over the entire electrode surface, and their interfaces between the active material and electrolyte are not easy to be extracted, making it difficult to measure ECSA.

In this study, to enable the measurement of ECSA in ASSB, we first construct an interface consisting only of an active material

Research Article
doi.org/10.1002/batt.202500092
Chemistry Europe
European Chemical Societies Publishing

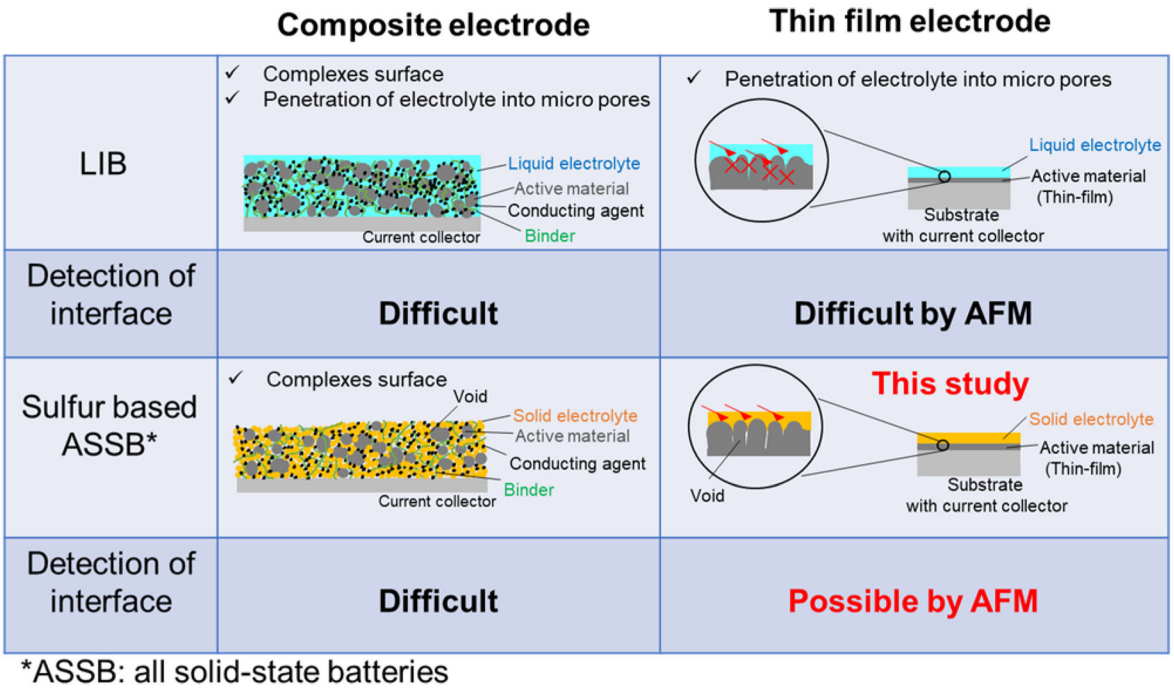

Figure 1. The comparison of cathode interfaces between LIB and sulfur-based all-solid-state batteries for composite electrodes and thin film electrodes.

thin film and an electrolyte. By using the active material thin film, the active material/electrolyte interface in ASSB becomes simple. In general, when two materials with different elastic moduli contact with each other at the interface, the surface shape of the material with the smaller modulus follows the one with the larger modulus. In other words, in case of an ASSB consisting of a sulfide solid electrolyte and oxide active material, the sulfide solid electrolyte deforms to match surface shape of the oxide active material thin film. This means that the interfacial contact area can be measured by surface analysis of the roughness of the active material thin film. Also, by measuring the capacitance at this contact interface, it is possible to correlate the capacitance with the interfacial contact area. Furthermore, by using an interface consisting only of an active material thin film and electrolyte, it is no longer necessary to consider the individual capacitance values of the active material, binder, and conducting agent, which must be considered separately in a normal composite electrode, and a direct association between the interface contact area and capacitance is possible. Based on the calibration curve obtained from this relation, it is possible to quantitatively determine the electrode ECSA of the composite electrode (which is difficult to define interface). In other words, ECSA of electrode can be read from capacitance of the active material at the interface of composite electrode (measurable by EIS), using the calibration curve as a clue. This report describes a concrete plan.

2. Results and Discussion

There are many parameters that affect film properties during cathode thin film deposition, including laser power, oxygen gas pressure, substrate temperature, distance between a target and a substrate, and target composition. In a previous report,[6] thin film NMC was successfully deposited on a substrate. The thin film NMC was polycrystalline and oriented only on the out-of-planes: NMC (003) plane // Pt (111) plane and not on the in-planes on the substrate. This allows for lithium-ion insertion and extraction capabilities similar to those of composite electrodes, without bias toward specific orientations seen in epitaxially grown single-crystal films,[7] and also maintains surface flatness. For details on the morphology and structure of the NMC thin film, please refer to the previous paper.[6] In the report,[6] depositions under various gas pressure as the parameter were investigated. As a result, NMC 003 diffraction ($2\theta = 8.59°$, Mo-Kα) intensity increased with increasing pressure from 0.01 to 10 Pa, and then decreased significantly at 20 Pa. In this study, all the deposition conditions were basically the same except for the oxygen gas pressure in each deposition. Therefore, the film properties changed depending on the gas pressure during deposition. **Figure 2** shows atomic force microscope (AFM) images of NMC films deposited at oxygen gas pressures of 9.2 and 11.2 Pa.

The higher gas pressure results in finer particles. This grain refinement improves specific surface area (SSA). Figure S1, Supporting Information, shows a cross-sectional transmission electron microscopy (TEM) image of the thin film. The thickness of each layer is 70 nm for the NMC film and 14 nm for the LNO film. Moreover, the composition of the NMC film was measured by inductively coupled plasma optical emission spectroscopy (ICP-OES) with Nb = 1, and Ni: Mn: Co = 0.34: 0.29: 0.29 (in molar ratio) while suggesting that the composition is almost NMC111.

Next, a typical Nyquist plot obtained from EIS measurement of a thin film cell is presented in **Figure 3**.

Figure S2, Supporting Information, also shows state of charge (SOC)-dependance of impedance of a thin film cell.

Research Article
doi.org/10.1002/batt.202500092
Chemistry Europe
European Chemical Societies Publishing

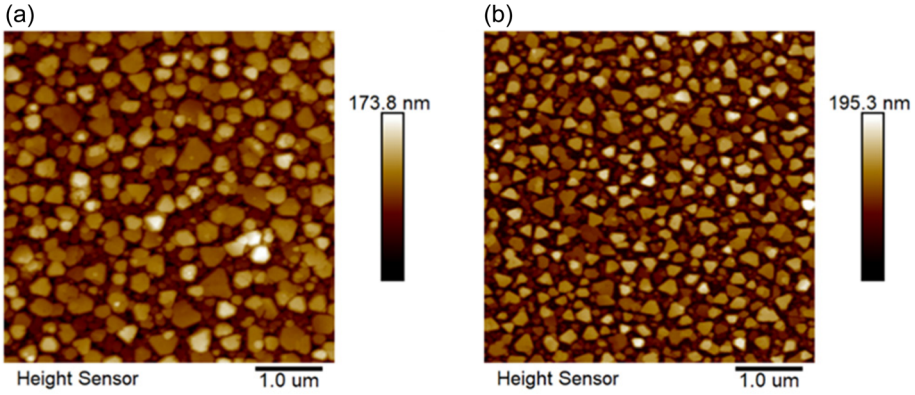

Figure 2. AFM topographic images for surface of NMC thin films produced at a) $PO_2 = 9.2$ Pa, and b) $PO_2 = 11.2$ Pa. SSA values calculated for (a) and (b), are 6.5 and 7.2 $m^2 g^{-1}$, respectively.

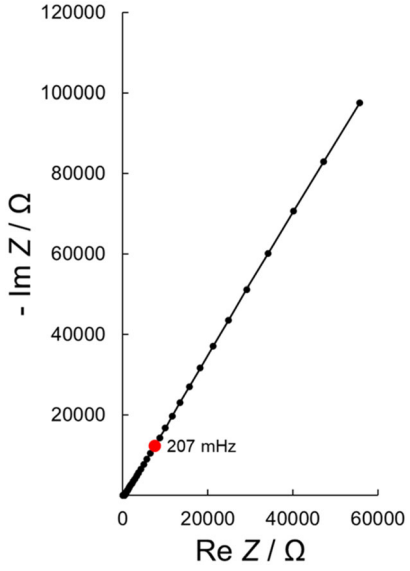

Figure 3. Nyquist pot of a thin film cell.

A characteristic shift of phase angle is observed in high frequency (R1, a peak frequency: 1.46 kHz, time constant: several milliseconds) in the Bode plot of Figure S2b, Supporting Information. A typical semicircle is not clearly found in the relevant frequency in the Nyquist plot of Figure S2a, Supporting Information, however, a sign of R1 is annotated for the purpose of explanation in both figures. R1 is attributed to resistance of an interface film formed by decomposition on the surface of a cathode.[8–11] Moreover, referring to previous reports,[6,12] judging from the ranges of time constants of charge transfer resistance (R_{ct}: several hundred milliseconds to several seconds) for a thin film cell, we assigned the semicircle (or shift of phase angle) of the following low frequency range to R_{ct}. To understand the details of the resistance changes for SOC in R1 and R_{ct}, equivalent circuit fitting was performed. Figure S3, Supporting Information shows the results. As expected with the increase in SOC, the interface film resistance of R1 showed almost no change, while R_{ct} exhibited a nonlinear L-shaped decrease in resistance with an increase in SOC up to 75%. This characteristic resistance change with respect to SOC is the same as the previous results obtained for the charge transfer resistance of liquid LIBs.[6,13–15] At the following relevant low frequency range containing of 207 mHz, a typical blocking condition is appeared in the Nyquist plot of Figure S2a, Supporting Information (in Figure 3, also). Aforementioned discussions in Figure 3 and S2, Supporting Information, are those from results of EIS measurements for a thin film cell as "full cell". From the point of view, it is necessary to separate a frequency range between cathode interface and anode interface to discuss as cathode interface about low frequency range containing of 207 mHz. Therefore, EIS measurements using thin film cells as "symmetric cell" were conducted. As clearly shown in Nyquist plot and Bode plot of Figure S4, Supporting Information, a profile of full cell almost coincides with that of cathode symmetric cell and is far different from that of anode symmetric cell (a peak frequency: 2.1 Hz). Hence, it is proved that C value at 207 mHz observed in full cell is originated from cathode interface. Consequently, current setup of thin film cell regards ECSA as information from cathode interface.

Results obtained from ten thin films are shown in **Figure 4**. A calibration curve prepared with specific capacitance of each

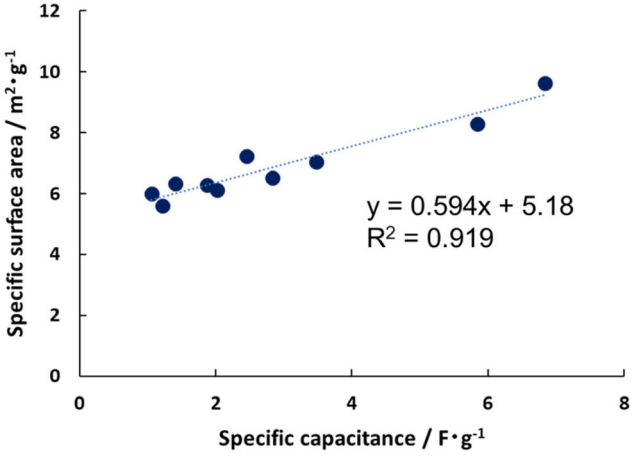

Figure 4. Calibration curve for thin film cells. This curve shows the relationship between specific capacitance and SSA of a thin film cell.

Research Article
doi.org/10.1002/batt.202500092
Chemistry Europe
European Chemical Societies Publishing

thin film cell on the horizontal axis and SSA of each thin film on the vertical axis is revealed.

It shows a linear relationship between specific capacitance and SSA. The expression of approximate line and the coefficient of determination (R^2) are shown in the figure (hereafter, the expression of approximate line is referred to as the thin film calibration curve). This thin film calibration curve reveals that the specific capacitances and SSA values are correlated with a slope of "0.594" due to the increase in roughness of the cathode active material at the interface between the electrolyte and the cathode active material. In contrast, *y*-intercept of the thin film calibration curve is "5.18". Here, the value of 5.06 $m^2\,g^{-1}$ is separately calculated using an electrode geometrical area when the film weight is the average value of the active material thin film: 16 μg. This value is very close to the *y*-intercept value. Namely, the *y*-intercept value reveals that the roughness of the active material formed on the substrate is zero.

Further supplementing the linear relationship between specific capacitance and SSA. The EIS measurements in this study were conducted at 0%-SOC after three discharge cycles using constant current constant voltage (CCCV). For comparison, the results conducted at 0%-SOC after four discharge cycles using CCCV for each cell are shown in Table S1 and Figure S5, Supporting Information. From Table S1, Supporting Information, it can be seen that the specific capacitance values at all plot points in the fourth cycle are reduced by almost the same proportion compared to the third cycle. Additionally, when the calibration curve is drawn using the values from the fourth cycle in Figure S5, Supporting Information, the same proportional relationship between specific capacitance and SSA as in Figure 4, which was drawn using the values from the third cycle, is obtained. This indicates that reproducible results can be obtained when comparing 0%-SOC values between cells with the same cycle history. Here, we discuss the acquisition of capacitance values in this study based on the imaginary axis *Z* values at specific frequencies. This is to investigate the impact of capacitance values based on various CPEs.[16] For comparison, instead of reading the imaginary axis *Z* values at specific frequencies, the results based on CPE obtained by fitting with R-CPE (CPEct in the equivalent circuit of Figure S6, Supporting Information) and CPE (CPE2 in the equivalent circuit of Figure S7, Supporting Information) are shown, respectively. In both cases, the slope of the calibration curve is 0.852, confirming that there is no difference based on the equivalent circuit used.

Next, complement about weight of thin film must be provided. Figure S8, Supporting Information shows a concept drawing for explanation of cathode interfaces for thin film electrodes. The thin film calibration curve must correlate roughness and capacitance in the interface. Namely, as shown in Figure S8a, Supporting Information, it is ideal that thin film is dominated by surface roughness only. If the contribution from film bulk not surface is significant, particularly the weight of the thin film is high, such as 21 μg, the contribution from the bulk cannot be neglected. For comparison with the actual experimental results, the calibration curves obtained at 14–21 μg after three discharge cycles and four discharge cycles are shown in Figure S9 and S10, Supporting Information, respectively. The red circles in each figure represent the newly added data points resulting from the expanded weight range. In both graphs, compared to the calibration curves in Figure 4 and S5, Supporting Information, created with cells in the 14–18 μg range, the specific capacitance values are observed to be distributed around 0.6–2 F g^{-1}, despite the cells being made with thin films of ≈5 $m^2\,g^{-1}$. As a result, a linear relationship is not obtained. Including these points in the calibration curve results in significant errors. This clearly indicates that the cells were formed with films of substantial weight. Accordingly, in this study, the weight of active material thin film is limited between 14–18 μg as average 16 μg and the calibration curve is constructed. By doing so, the influence from film bulk can be neglected.

Next, ECSA of the composite cell is estimated based on the thin film calibration curve. The calibration curve for the composite cell is shown in **Figure 5**.

Here, the *y*-intercept is replaced *y*-intercept of the thin film cell: the roughness zero value (5.18 $m^2\,g^{-1}$) in new *y*-intercept value, the roughness zero value of the composite cell. The zero-roughness value of the composite cell is calculated as 0.0105 $m^2\,g^{-1}$ from the active material weight of 7.5 mg and the electrode geometrical area. By the same manner, to get the specific capacitance of a thin film cell, the specific capacitance of the composite cell was determined at 0%-SOC using EIS measurement, and 0.0154 F g^{-1} was obtained. As shown in the Figure 5, extrapolating the calibration curve, and substituting the above-mentioned *x* value of 0.0154 F g^{-1} for the calibration curve of the composite cell: $y = 0.594x + 0.0105$, SSA of the composite cell of 0.0196 $m^2\,g^{-1}$ (namely, ECSA) is obtained. Further supplementing the ECSA measurement of composite cells using the calibration curve. As mentioned earlier, in this study, the specific capacitance value was obtained based on the imaginary axis *Z* values at specific frequencies. When fitting with R-CPE (CPEct in the equivalent circuit of Figure S6, Supporting Information) and CPE (CPE2 in the equivalent circuit of Figure S7, Supporting Information), instead of reading the imaginary axis *Z* values at specific frequencies, the slope of the calibration curve based on CPE was 0.852 in both cases. Even if the slope is changed

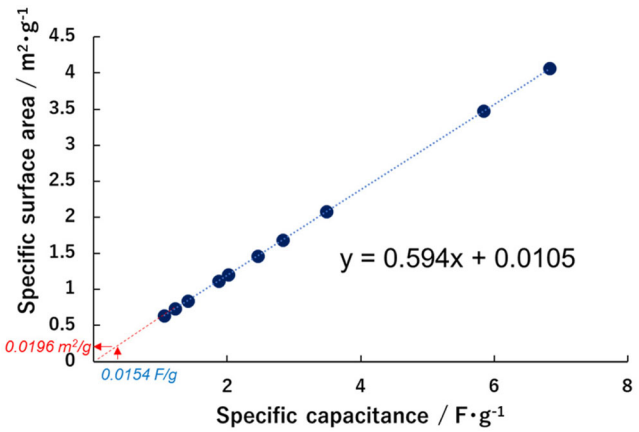

Figure 5. A calibration curve for ASSBs with composite cathode electrodes. Based on a specific capacitance measured at the cathode electrode, SSA (namely, ECSA) is obtained from this curve.

to 0.594 based on the capacitance of the imaginary axis *Z* values, and the above ECSA is calculated using the slope (0.852) as the standard, a similar value of 0.0237 $m^2 g^{-1}$ is obtained.

The validity of ECSA of the composite cell is discussed. As an example, a SSA of the composite cathode of liquid LIB using BET method is reported to be the range between 1.1 and 1.8 $m^2 g^{-1}$.[4,17] The weights for the calculation of BET surface area are normally based on total electrode weights, not weights of only active material. If the values convert to the weights of active material, as an example of 75 wt% used in this study, 1.1 and 1.8 $m^2 g^{-1}$ is 1.5 and 2.4 m^2 g-AM^{-1}, respectively. In a previous report[18] for liquid LIB, they noted that ECSA is 0.4 m^2 g-AM^{-1} using normalized capacitance based on electrode geometrical area (28 $\mu F cm^{-2}$) and specific capacitance (0.125 F g-AM^{-1}). It shows that ECSA for Liquid LIB is smaller than BET surface area of a composite electrode in liquid LIB. For a reference, using the reported normalized capacitance based on electrode geometrical area (28 $\mu F cm^{-2}$) for liquid LIB and the specific capacitance obtained in this study (0.0154 F g^{-1}), the ECSA is calculated to be 0.0550 m^2 g-AM^{-1}. This value is of the same order of magnitude as the value (0.0196 $m^2 g^{-1}$) obtained in this study. As is shown in Figure 1, unlike liquid electrolytes, it is difficult for solid electrolytes to get into the microstructure, it is reasonable that ECSA (0.0196 $m^2 g^{-1}$) obtained for solid electrolyte LIB in this study is smaller than the value (0.4 $m^2 g^{-1}$) reported previously for liquid LIB.[18]

3. Conclusions

A simple active material/electrolyte interface using a cathode active material thin film has been constructed to enable the measurement of ECSA in all-solid-state batteries. The interfacial contact area has been quantified by AFM analysis of the roughness of the active material thin film, since the solid electrolyte deforms to the surface profile of the oxide-based active material thin film (NMC) due to the low elastic properties of the sulfide-based solid electrolyte. At the same time, the capacitance at the interface has been measured from EIS measurements of thin film cells, and the correlation between specific capacitance and specific contact area has been investigated. Consequently, specific capacitance and specific contact area have a linear relationship to make calibration curve. Using this calibration curve as a clue, the interfacial contact area (namely, ECSA) of a composite electrode, which was previously difficult to define the interface, can be quantitatively determined from the specific capacitance value which can be easily obtained by EIS measurement of the composite cell.

4. Experimental Section

Preparation and Characterization of Cathode Thin Films

A thin film of cathode active material: NMC was formed by pulsed laser deposition using an neodymium-doped Yttrium aluminum garnet (Nd-YAG) laser (wavelength: 266 nm). The fabrication procedures were previously reported.[6] As a substrate, a single-crystal silicon (Si) substrate (9 mm × 9 mm, 0.5 mm in thickness) was sputter-deposited with a base chromium (Cr) layer and a platinum (Pt) current collecting layer (total 50 nm in thickness) on both sides and the lateral whole of the substrate to provide current collection properties as an electrode. NMC film was formed on Cr/Pt layers as only one side of the substrate; the target for NMC film deposition was a sintered material of NMC with a lithium excess composition ($Li_{1.5}Ni_{1/3}Co_{1/3}Mn_{1/3}O_2$, Toshima Corporation). Deposition to form the NMC film was conducted under the following conditions: oxygen gas pressure of 8–12 Pa, temperature of 923 K, deposition time of 50 min, laser power of 200 mW, and repetition frequency of 10 Hz. For making a low interfacial resistance with sulfide SE,[19] a film (LNO film) using a sintered lithium niobate target ($LiNbO_3$, Toshima Corporation) was deposited as a coating layer on the NMC film by changing the temperature to 673 K and the deposition time to 15 min from the deposition conditions for NMC film. The thin film substrate after deposition was weighed using a precision balance (BM-5, AND), and the weight of the active material in a thin film substrate was determined as difference from the weight of the substrate before deposition. The weight measurements were performed several times before and after deposition each, and the average weight of the film was obtained. A cross-sectional sample of the thin film substrate was prepared using mechanical thinning, dimpling, and argon-ion milling. The cross-sectional image was acquired using TEM (TEM, JEOL JEM-ARM200F) operated at 120 kV. ICP-OES (ICP-OES, Hitachi PS3520VDDII) measurements were carried out for capturing composition of NMC layer on the thin film substrate.

Measurement of Surface Area of the Cathode Thin Films

Roughness images of the cathode active material thin film were acquired using an AFM (AFM, Dimension FastScan, Bruker). The tapping mode with a silicon nitride cantilever (SCANASYST-AIR, k: 0.4 N m^{-1}) was conducted. Scans of 256 lines were carried out for 5 $\mu m \times 5 \mu m$ area at a scan speed of 1 Hz. The surface area of the thin film was calculated based on the average roughness value (*Ra*) of each roughness image obtained at several different locations on the substrate. Using the following Equation (1).

$$\text{Surface area of the thin film} = \frac{Sa * Sb}{Sc} \quad (1)$$

Sa: electrode geometrical area: 81 mm^2

Sb: image surface area, e.g., 32 μm^2 (surface area measured using AFM). This value was obtained using NanoScope Analysis software by Bruker.

Sc: scan-setting area for AFM measurements: 25 μm^2

The averaged surface area value was divided by the cathode active material film weight (typically, 16 μg) to obtain the SSA value ($m^2 g^{-1}$).

Preparation of Sulfide Sold Electrolytes

Reagent-grade lithium sulfide (Li_2S) powder, phosphorus pentasulfide (P_2S_5) powder, and lithium chloride (LiCl) powder were weighed in a 4:1:3 molar ratio and dry-mixed at 240 rpm for 30 h using a planetary ball mill (Pulverisette 7, Fritsch). The mixed powder was then calcined in a tube furnace at 823 K for 2 h under argon gas environment. The sample was then crushed in a mortar and sieved through a 25 μm sieve to obtain a powdered sulfide solid electrolyte (composition: $Li_{5.5}PS_{4.5}Cl_{1.5}$, hereafter SE).

Preparation of Thin Film Electrochemical Cells

A thin film electrochemical cell (φ 16 mm, hereafter referred to as thin film cell) was prepared using a thin film electrode and

powdered electrolyte. The active material thin film was used as the cathode, and a lithium-indium alloy (Li-In foil) was used as the counter electrode. A piece of 2.6 mg of lithium foil (thickness: 200 μm, Honjo Metal Co., Ltd.) and 130 mg of indium foil (thickness: 100 μm, Niraco Corporation) were punched out in a diameter of 15 mm and laminated to prepare In_3Li alloy in following procedure (hereafter, Li-In foil).[20] Powdered SE was used as the electrolyte. The thin film cell fabrication procedure as follows. First, the active material thin film was put into the cell. Next, 250 mg of SE powder was added, and a forming pressure of 290 MPa was applied using a uniaxial dry press. Then, the shaft on the opposite side of the cathode was removed, a Li-In foil was attached, and a forming pressure of 115 MPa was applied again. Furthermore, two restraining jigs were bolted down in 1.6 MPa at both ends of the cell, and finally, the cell was further set in a special container for nonexposure to air to prepare a thin film cell as full cell. Schematic drawing of the thin film cell is available in Figure S11a, Supporting Information. A positive electrode (cathode) symmetric cell was created by changing the negative electrode to the positive electrode in the above full cell, and a negative electrode (anode) symmetric cell was prepared by changing the positive electrode to the negative electrode in the above full cell. The fabrication of thin film cells was carried out in an argon gas environmental glove box.

Measurement of Specific Capacitances of the Interface Using EIS

Capacitances of the interface were measured by EIS. After ageing for Li–In alloying for six hours at 298 K, as an initial conditioning cycle of the thin film cell, three cycles of charge and discharge were carried out at 1 μA between 2.08 and 3.68 V (vs Li–In) using galvanostatic cycling with potential limitation (GCPL) program of the EC-Lab software using a multipotentiostat/galvanostat (VMP3, BioLogic). The discharge capacity of the third cycle was measured and the C rate was calculated (typically, 1C = 1 μA). EIS measurements were then carried out using a following procedure on the same instrument. First, the thin film cell was discharged at 0.1 C to 2.08 V using GCPL program, then further discharged with constant voltage at 2.08 V until the current decayed to 0.01 C. At the resulting 0%-SOC after a three-hour rest, EIS measurements were performed at 2.08 V (vs Li-In). potensiostatic EIS (PEIS) program of EC-Lab software was used for EIS measurements using the following conditions: 1MHz–10 mHz (as frequency range) with ten points per decade and 10 mV (AC voltage perturbation). Both conditioning and EIS measurements of the thin film cells were carried out in a thermostatic chamber at 298 K.

The method for obtaining the capacitance at 0%-SOC (as blocking state at cell interface) referred to Equation (2) of a previous report.[4]

$$Q \approx \frac{1}{\omega_0(-\mathrm{Im}(Z\omega_0))} \tag{2}$$

The above ω_0 and Q are the specific angular frequency [rad/s] and constant phase element (CPE) [$F/s^{1-\alpha}$], respectively. α is phase angle ($0 < \alpha < 1$). In the above equation, Q agrees with $\omega_0 \approx 1\ s^{-1}$ when the specific frequency $f_0 = 200$ mHz and $\alpha > 0.79$. Then, Q is equivalent to a capacitor.[4] In this study, values at $f_0 = 207$ mHz to obtain Q are used, which is the closest to 200 mHz reported in the reference.[4] Also, typical measured value is $\alpha = 0.80$ (i.e., See a Nyquist plot in Figure 3). They satisfy the above condition. Consequently, the capacitance was obtained from Z'' ($= -\mathrm{Im}\ Z$) value at 207 mHz. Finally, the capacitance (F) was divided by the cathode active material film weight (typically, 16 μg) to obtain specific capacitance (F/g).

Preparation of All-Solid Cells Consists of Composite Electrodes and Measurement of Their Specific Capacitances Using EIS

In this study, a composite cathode was prepared only of an active material and SE to avoid the influence of a conductive agent and a binder. First, for making the composite cathode, active material powder ($LiNbO_3$-coated NMC111) and SE were mixed at a ratio of 75:25 (wt%) in a mortar. After mixing in a mortar, the powder was put in a glass vial bin and further mixed with an automatic stirrer. The preparation procedure for all-solid electrochemical cell using the composite electrode (composite cell) as follows. First, SE powder (80 mg) was put in the electrochemical cell (φ10 mm) and a forming pressure equivalent to 37 MPa was applied. Next, a long shaft of the electrochemical cell was taken off once, the composite cathode (10 mg) was put into the cell, then, the long shaft was put back and a forming pressure equivalent to 293 MPa was applied. Then, a short shaft on the opposite side of the cathode was removed, Li-In foil (47 mg) punched out in diameter of 9 mm was attached on the shaft of the anode, then, the short shaft was put back and 110 MPa was applied. Furthermore, two restraining jigs were bolted down in 1.5 MPa at both ends of the cell, and finally, the cell was further set in a special container for nonexposure to air to prepare as a composite cell. Schematic drawing of the composite cell is available in Figure S11b, Supporting Information. The fabrication of composite cells was also carried out in an argon gas environmental glove box.

The capacitance of the composite cell was obtained at 298 K by EIS measurement using the same protocol as the thin film cell except for the current using 0.05 C (as 1 C = 1 mA). The capacitance value was divided by the weight of the cathode active material (7.5 mg) to obtain the specific capacitance value (F/g) of the composite cell.

Acknowledgements

The author gratefully acknowledges Dr. Yasushi Maeda (AIST) for helping in AFM analysis and fruitful discussions. This work was supported by Honda R&D Co., Ltd.

Conflict of Interest

The authors declare no conflict of interest.

Data Availability Statement

The data that support the findings of this study are available from the corresponding author upon reasonable request.

Keywords: electrochemical impedance spectroscopy · electrochemically active surface area · solid-state lithium-ion battery · specific capacitance · thin-film cell

[1] A. A. France, *RSC Adv.* **2017**, *3*, 13027.
[2] J. J. F. Scholten, *Stud. Surf. Sci. Catal.* **1979**, *3*, 685.
[3] T. Binninger, E. Fabbri, R. Kötz, T. J. Schmidt, *J. Electrochem. Soc.* **2014**, *161*, H121.
[4] S. Oswald, D. Pritzl, M. Wetjen, H. A. Gesteiger, *J. Electrochem. Soc.* **2020**, *167*, 100511.
[5] H. Li, J. Lampkin, Y. Chien, L. Furness, D. Brandell, M. J. Lacey, N. Garcia-Araez, *Electrochim. Acta* **2022**, *403*, 139572.

[6] T. Ohashi, T. Hirano, K. Okazaki, T. Fukunaga, T. Abe, *J. Electroanal. Chem.* **2021**, *899*, 115675.
[7] M. Hirayama, M. Abe, S. Taminato, Y. Araki, K. Suzuki, R. Kanno, *RSC Adv.* **2016**, *6*, 78963.
[8] M. Itagaki, N. Kobari, S. Yotsuda, K. Watanabe, S. Kinoshita, M. Ue, *J. Power Sources* **2005**, *148*, 78.
[9] S. S. Zhang, K. Xu, T. R. Jow, *Electrochem. Solid-State Lett.* **2002**, *5*, A92.
[10] D. Aurbach, M. D. Levi, E. Levi, H. Teller, B. Markovsky, G. Salitra, L. Heider, U. Heider, *J. Electrochem. Soc.* **1998**, *145*, 3024.
[11] D. Aurbach, K. Gamolsky, B. Markovsky, G. Salitra, Y. Gofer, *J. Electrochem. Soc.* **2000**, *147*, 1322.
[12] L. Zhang, Y. Dai, C. Li, Y. Dang, R. Zheng, Z. Wang, Y. Wang, Y. Cui, H. Arandiyan, Z. Shao, H. Sun, Q. Zhuang, Y. Liu, *Energy Storage Mater.* **2024**, *69*, 103378.
[13] V. Charbonneau, A. Lasia, G. Brisard, *J. Electroanal. Chem.* **2020**, *875*, 113944.
[14] T. Ohashi, T. Abe, T. Fukunaga, Z. Ogumi, E. Matsubara, *J. Electrochem. Soc.* **2020**, *167*, 020502.
[15] T. Ohashi, K. Okazaki, T. Fukunaga, Z. Ogumi, T. Abe, *ChemElectroChem* **2020**, *7*, 1644.
[16] G. J. Brug, A. L. G. van den Eeden, M. Sluyters-Rehbach, J. H. Sluyters, *J. Electroanal. Chem.* **1984**, *176*, 275.
[17] E. Trevisanello, R. Ruess, G. Conforto, F. H. Richter, J. Janek, *Adv. Energy Mater.* **2021**, *11*, 2003400.
[18] S. Oswald, F. Riewald, H. A. Gesteiger, *J. Electrochem. Soc.* **2022**, *169*, 040552.
[19] N. Ohta, K. Takada, I. Sakaguchi, L. Zhang, R. Ma, M. Fukuda, M. Osada, T. Sasaki, *Electrochem. Commun.* **2007**, *9*, 1486.
[20] S. Luo, Z. Wang, X. Li, X. Liu, H. Wang, W. Ma, L. Zhang, L. Zhu, X. Zhang, *Nat. Commun.* **2021**, *12*, 6968.

Manuscript received: February 10, 2025
Revised manuscript received: April 9, 2025
Version of record online: April 15, 2025